Theoretical study of native defects in III-V semiconductors

P. J. Lin-Chung and T. L. Reinecke
Naval Research Laboratory, Washington, D.C. 20375
(Received 10 May 1982)

The local densities of states associated with antisite and vacancy defects in the III-V semiconductors GaAs, GaP, InP, InAs, and AlAs have been studied using the large-cluster recursion approach of Haydock, Heine, and Kelly. The resonant states and localized states induced by these native defects and the associated electron-charge redistributions are calculated and discussed. The principal states in the fundamental energy gaps corresponding to these defects are found to be the following: for ideal cation vacancies, localized T_2 states in the lower parts of the gaps, for ideal anion vacancies, T_2 states in the upper parts of the gaps, and for anion antisite defects, states of A_1 symmetry in the upper parts of the gaps. For cation antisite defects in AlAs and GaAs, no gap states are found. An ideal divacancy in GaAs is found to introduce four gap states. The properties of intrinsic defects near an ideal GaAs-AlAs (100) interface also have been studied. It is found that the interface does not affect the general features of the local density of states induced by the defect. The total electronic energies of interaction between the defects and the interface are calculated by a generalized zeros-and-poles method, and the resulting interactions between the defects and the interface indicate that nonstoichiometry may result there.

I. INTRODUCTION

Defects which introduce "deep" electronic states with ionization energies of the order of the width of the band gap are thought to be a main factor limiting semiconductor device performance and reliability. In III-V semiconductors, vacancies, interstitial defects, and antisite defects represent the basic native defects which produce nonstoichiometry and deep localized levels. In binary compounds, an anion (cation) antisite defect is formed when an anion (cation) occupies a cation (anion) site. This occurrence is favored when the differences in size and electronegativity between the two constituent atoms are small. Thus, in principle, it is more favorable in GaAs than in GaP.

Experimental evidence for anion (cation) antisite defects has been reported for binary semiconductors in which the cation (anion) has more shells of electrons than the anion (cation). Examples are the anion antisite in GaP (Refs. 1–5) and in GaAs (Refs. 6 and 7) and cation antisites in GaSb (Ref. 8) and AlSb (Ref. 9). ESR gives strong evidence for the identity of the defect center from its characteristic nuclear-spin hyperfine-structure and ligand hyperfine-structure patterns. The absolute position of the energy levels of the deep centers generally have not been determined experimentally, however. Several levels ($E1$, $E2$, $E3$, $E4$, $E5$, and $H1$), which are detected by deep-level transient spectroscopy in GaAs,[10] have not yet successfully been identified with specific types of defects.

There has been increasing interest in theoretical investigations of native defects in the III-V materials in recent years.[11–15] Scheffler *et al.*[11] and Bernholc and Pantelides[11] carried out self-consistent pseudopotential Green's-function calculations on native defects in GaP. Their results support the identification of the antisite given in ESR studies but contradict the identification of cation vacancy in GaP. They attribute the ESR spectrum previously attributed to the Ga vacancy to carbon at Ga sites. However, more recent work by Kennedy and Wilsey[16] does not agree with the carbon identification for experimental reasons. Because of the controversy existing in the current literature, more comprehensive investigations of the deep centers is desirable.

Other areas of importance concerning the defect problem are the defect interaction with an interface and the defect-defect interaction. These effects form the basis of understanding the likelihood of the formation of certain defect complexes and can provide information about the selective diffusion of defects. Previously there have been some suggestions concerning the existence of defect complexes in III-V semiconductors.[8] Diffusion of defects has also been observed across semiconductor-semiconductor interfaces.

To investigate the deep-center problem theoretically, various approximate methods are being used. In the case of III-V compounds, use has been made of the pseudopotential method[12] and of empirical variants of the Green's-function method.[11] These

methods have a number of shortcomings, including a considerable amount of computation time required in carrying out k-space integrations and difficulties in determining the local parameters of deep centers.

In the present work, we employ a continued-fraction recursion method which has been applied successfully to amorphous materials and to the surface-adsorption problem.[17] We find that this method is especially useful in dealing with localized states in semiconductors. Previously this method has been applied to study defect states in semiconductors in a preliminary way using smaller clusters[18] or limited expansion of the continued-fraction expressions.[15] In the present work we examine carefully the convergence of the results and the effects of the tight-binding interatomic interactions on the results. Based on this continued-fraction approach, a new formalism[19] is adapted here to evaluate the defect-interface interactions. Details of the present method will be discussed in the next section. Section III gives our calculated results for vacancy and antisite defects in a series of III-V semiconductors and for defects near a model GaAs-AlAs interface. Section IV is a summary of the work. Preliminary reports of some aspects of these results have been published in Ref. 20.

II. THE CALCULATIONAL METHOD

There are a number of methods for solving the Schrödinger equation for the case of a deep impurity in a semiconductor. Early interpretation of the experimental results for transition-metal impurities in III-V semiconductors relied upon crystal-field theory. However, this approach does not provide a satisfactory quantitative theory because the approximations involved do not allow for the effect of covalent bonding. Subsequently, theoretical analyses of deep-center energy spectra employed the pseudopotential method,[12,13] the small-cluster augmented-plane-wave method,[21] the scattering theoretical method[11] and self-consistent Green's-function techniques.[22] All of these methods make use of the perfect periodicity of the unperturbed system to simplify the computation. Thus they have limited capabilities in studies of many important aspects of deep-center problems, for example, for deep defect centers near surfaces and interfaces where periodicity is substantially altered, for defects in the presence of lattice relaxation, or for extended defect complexes.

When a deep defect center or a cluster of defects is incorporated into a bulk solid or solid surface, it is logical to seek an approach which is not based on the translational symmetry of the lattice but rather is based on the local atomic environment. The recursion method provides such an approach. It does not utilize k-space representations at all even where there is lattice periodicity. Therefore, one need consider only the real-space Green's function. The attractive features of this method as compared with alternative approaches can be summarized as follows:

(1) It does not require crystal periodicity to simplify the calculation. Thus the existence of surfaces, interfaces, or lattice distortions can be incorporated without additional complexity.

(2) Three points related to calculational efficiency are as follows:

(a) In the local atomic environment approach to solid-state physics, the Hamiltonian of a large cluster has a matrix that is usually too large to store in the computer, but its matrix elements are simple to compute. The recursion method has the advantage of computing with vectors from the space operated on by the Hamiltonian but not by the matrices. Therefore, there is no need to store a large matrix and no restriction on the size of the cluster on this account.

(b) The recursion relation is an easy algorithm to program. With the existing Cambridge Recursion Method Library routines, the computer time required to obtain the density of states of pure GaAs by this method using a cluster of 512 atoms is an order of magnitude less than that from a pseudopotential k-space integration method. The results, on the other hand, agree well with the pseudopotential calculations.

(c) Because of the calculational efficiency, this method is suitable for a large-cluster system. Unlike the small-cluster approach, surface effects become irrelevant in such a large cluster, and there is no difficulty in locating the band edges. However, it should be noted that one should be particularly careful in choosing the shape of the cluster when the recursion calculation is performed. As mentioned in Ref. 17, a regularly shaped cluster tends to add up boundary corrections from all parts of the boundary coherently in phase at the center. Thus one finds that even for a sufficiently large cluster, the boundary will introduce some spurious resonance peaks in the local density of states (LDOS) curve for the central atom if one chooses a spherical cluster. This can be eliminated by using a cluster with a shape as irregular as possible while retaining the symmetry of the Hamiltonian.

(3) The generalized "zeros-and-poles" method[19] which has been developed recently based on the recursion approach is useful for calculating very small differences in the total energy between two similar large aggregates of atoms with a sufficient accuracy to extract useful information. Therefore, it becomes feasible to study the interaction energy involving defects within the bulk, and at interfaces or surfaces.

In the recursion method one exploits the sparseness of the representation of a tight-binding Hamiltonian H and performs a unitary transformation on the local-orbital basis $|\alpha R_l\rangle$ to produce a tridiagonal representation of the Hamiltonian. Here $|\alpha R_l\rangle$ represents the state of the αth orbital of an atom at R_l site. New normalized basis functions $|U_n\rangle$ are then defined iteratively so as to guarantee that each new member interacts only with the preceding and following members, i.e.,

$$|U_0\rangle \equiv |\alpha R_l\rangle , \tag{1a}$$

$$b_n |U_n\rangle = (H - a_{n-1})|U_{n-1}\rangle - b_{n-1}|U_{n-2}\rangle , \tag{1b}$$

$$\langle U_n | U_n\rangle = 1 . \tag{1c}$$

After the transformation, the tridiagonal representation of the Hamiltonian matrix takes the following form:

$$\langle U_m | H | U_n\rangle = \begin{cases} a_m, & n=m \\ b_{m+1}, & n=m+1 \\ b_m^*, & n=m-1 \\ 0, & \text{otherwise} . \end{cases} \tag{2}$$

The matrix elements a_i,b_i are related directly to the continued-fraction coefficients in the expansion of the real-space Green's function $G_{\alpha l\alpha l}(E)$:

$$G_{\alpha l\alpha l}(E) = \langle \alpha R_l | [E-H]^{-1} | \alpha R_l\rangle = \cfrac{1}{E-a_0-\cfrac{b_1^2}{E-a_1-\cfrac{b_2^2}{E-a_2-\cfrac{b_3^2}{E-\cdots}}}} . \tag{3}$$

As a result, the matrix elements in Eq. (2) give the complete description of $G_{\alpha l\alpha l}(E)$, which in turn gives the physical quantities characterizing the system such as the local density of states $N_{\alpha l}(E)$ for the αth orbital at R_l site, the electronic occupancy $n_{\alpha l}$ of the $|\alpha,R_l\rangle$ state, and the total energy U of the system via

$$N_{\alpha l}(E) = -\pi^{-1} \operatorname{Im}_{\epsilon\to 0} G_{\alpha l\alpha l}(E+i\epsilon) , \tag{4}$$

$$n_{\alpha l} = \int_{-\infty}^{E_F} N_{\alpha l}(E)dE , \tag{5a}$$

$$U = \int_{-\infty}^{E_f} (E-E_F) N_{\alpha l}(E)dE . \tag{5b}$$

This real-space approach is especially useful because the action of the Hamiltonian on a particular orbital at a particular site can be considered independently in Eqs. (1)—(3), and thus the contribution from each orbital to the physical properties of the system can be obtained separately. The continued-fraction coefficients a_i,b_i given by Eq. (2) are related to the $(2i)$th-power moments of the LDOS as a function of energy. Therefore, the recursion method is analytically equivalent to computing the moments. These a_i,b_i are found to converge to constant values for increasing i. The constant a_i,b_i for large i gives the correct analytical spectrum $[E-E(\text{edge})]^{1/2}$ near the band edges, and the a_i,b_i for small i modulate the semielliptical spectrum with the local information extracted from H. It should be noted that for clusters of finite size the a_i,b_i for large i deviate substantially from the corresponding moments in the infinite cluster. This occurs when more and more paths which contribute to the a_i,b_i lie outside the boundary of the finite cluster. Thus care should be taken in practice concerning where to terminate a_i,b_i.

The convergence of the recursion approach has been examined in detail in the review articles in Ref. 17 for clusters of narrow—d-band transition metals. In semiconductor systems the second-neighbor interactions become more important than in the case of transition metals, and therefore we have examined the convergence of the present calculations carefully.

The atomic-orbital basis functions $|\alpha R_l\rangle$ in Eq. (1) are chosen to be orthonormal in this calculation. The tight-binding Hamiltonian matrix elements are then related to the Slater-Koster parameters as will be discussed in Sec. III A. To examine the convergence of the calculation for a given set of Slater-Koster interaction parameters which reproduce the bulk energy bands accurately for GaAs, we vary N, the size of the cluster, and L, the length of the continued-fraction expansion. The a_i,b_i are calculated explicitly for $i=1$ to $i=L$. The results for the density of states (DOS) of such GaAs clusters are displayed in Fig. 1.

Because the N and L constitute independent sources of approximation, one must select the size of the cluster and the length of a_i,b_i of the expansion to produce the most accurate results consistent with given computing resources. As seen in Fig. 1, the best agreement with the pseudopotential results of Chelikowsky and Cohen[23] is for the cases $N=216$, $L=19$, and $N=512$, $L=25$. With second-neighbor interactions taken into account, the minimum number of interaction steps from the central atom to the boundary of the clusters is four for $N=512$. According to an empirical rule of thumb,[17] the recursion then should be carried to $L\simeq 8$. However, because the total bandwidth W of the semiconductor

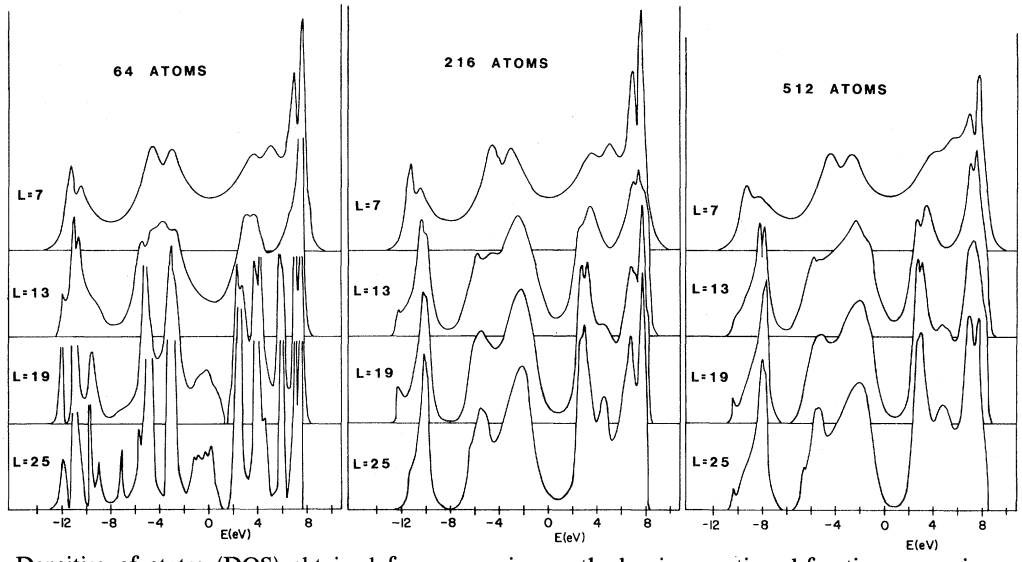

FIG. 1. Densities of states (DOS) obtained from recursion method using continued-fraction expansions of lengths $L=7,13,19,25$ for pure GaAs clusters of 64, 216, and 512 atoms.

GaAs is rather wide (~ 24 eV), L must have a higher value in order to achieve a better energy resolution which is proportional to W/L.

Our calculations shown in Fig. 1 indicate that the LDOS of a cluster containing 64 atoms deviates substantially from the pseudopotential calculation, and thus a cluster of size less than 200 atoms does not give a reliable approximation for the bulk crystal. On the other hand, there is no significant difference between the LDOS of clusters containing 216 and 512 atoms, and they all agree with the pseudopotential results quite well. [See Ref. 20(a), Fig. 1a.] We conclude that the 512-atom cluster has reached the desired convergence for the accurate representation of the bulk crystal. Also shown in Fig. 1 are the effects of increasing L, the length of the continued-fraction coefficient. For a 64-atom cluster and $L=19$ and 25, the LDOS contains many resolved δ-function distributions near the band edges. This is consistent with the explanation that the resolution of individual levels moves in from the extremes of the spectrum as L increases.[17] For even larger L, the LDOS turns into a complicated series of spikes.

Although the LDOS is not a stable convergent function of E, the physical quantities in which we are interested are satisfactorily convergent with increasing size of cluster.[17] Such physical quantities are represented by integrals over all the states of the system as given by Eq. (5). Indeed, the problem of stability and convergence does not affect localized states as much as extended states, and this also helps to justify the use of the present approach for the investigation of deep levels. The numerical uncertainty of the cation vacancy level in GaAs, for example, is found to be ± 0.12 eV for $L>19$ and $N=512$ atoms.

In Fig. 2 we show the convergence of the integrated quantities of Eqs. (5a) and (5b) with respect to the size of the cluster and the length of the continued-fraction expansion for the pure GaAs cluster described above. The convergence of the total energy in Eq. (5b) has been reached for $L>19$ and

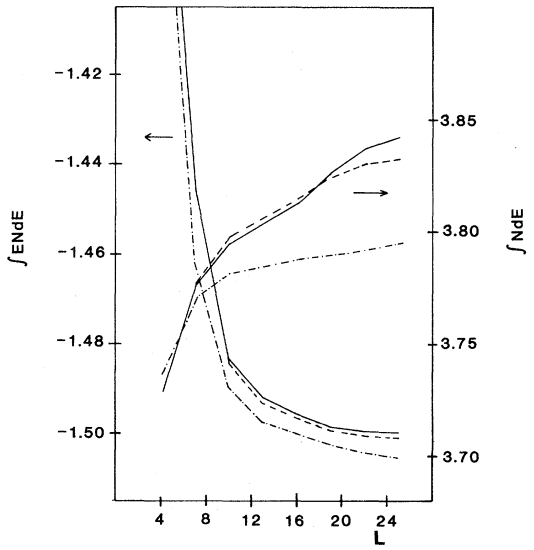

FIG. 2. Test of convergence of the integrated quantities of the local density of states in GaAs when the length L of continued-fraction coefficients changes. $\int N\,dE$ is the number of electrons, and $\int EN\,dE$ is the total electronic energy at one site. Solid curve, dashed curve, and dash-dotted curve are for clusters of 512, 216, and 64 atoms, respectively. The energies are in rydbergs.

$N > 216$ atoms. The difference in this energy for 216 and 512 atoms evaluated at $L > 19$ is less than 0.015 eV.

In this method, a rudimentary form of self-consistency in LDOS calculations can be used to provide the correct total electron occupancy of the atoms and a uniform Fermi energy in a solid. In general, for a defect or impurity the local potential is a strong function of the charge transfer into the impurity orbitals with a resulting change in the local potential which must be incorporated into a new calculation of all the LDOS until the correct total electron occupancy is achieved for a given Fermi energy. A simple scheme involving the changes of self-energies alone can be used to capture the essential physics. In this way in more elaborate calculations the local hopping integrals are also changed.

In order to determine the interaction energies between defects or between defects and surfaces or interfaces, we utilize a generalized zeros-and-poles method.[19] The interaction energy is the small change of total electronic energy of the system when a defect is introduced in the vicinity of another defect or a surface. The introduction of a defect in a large system produces a local perturbation and hence a very small change in the total electronic energy of the system. The subtraction of two large quantities arising from the total energies before and after the perturbation to obtain a small quantity in general will give rise to a large uncertainty. Moreover, when a local perturbation is turned on, the local density of states at not only the perturbed site changes, but also the local density of states over a large volume surrounding the perturbed site will change. This can be due to charge transfer or to the relaxation of atoms in the neighborhood of the defect. Under such conditions, the summation over all the local densities of states to obtain the total density of states becomes impractical. A new formalism designed to circumvent the above difficulty is used here. This formalism gives the change of the total energy directly without the necessity of finding the total densities of states of the system before and after the local perturbation. The formalism is exact. The only approximations occur in the modeling of the solid via a tight-binding cluster.

In the tight-binding picture, the change of the total density of states of the system for complex energies E can be expressed as

$$\begin{aligned}\Delta N(E) &= N(E) - N_0(E) \\ &= \mathrm{Tr}G - \mathrm{Tr}G_0 \ . \end{aligned} \tag{6}$$

Using the identity

$$\mathrm{Tr}(EI-H)^{-1} = \frac{\partial}{\partial E}[\ln \det(EI-H)] \tag{7}$$

and the relation from the theory of determinants

$$(\det M)^{-1} = \prod_{i=1}^{s} [(M_{i-1})^{-1}]_{11} \ , \tag{8}$$

where M is a square matrix of order s, and M_{i-1} represents a matrix formed by deleting the first $i-1$ rows and columns of M, and

$$[(M_{i-1})^{-1}]_{11}$$

is the (1,1) element (at the upper left-hand corner) of the matrix $(M_{i-1})^{-1}$, we obtain

$$\Delta N(E) = \sum_{i=1}^{nm} \frac{\partial}{\partial E} \ln \frac{\{[(EI-H_0)_{i-1}]^{-1}\}_{11}}{\{[(EI-H)_{i-1}]^{-1}\}_{11}} \ . \tag{9}$$

H_0 and H are the Hamiltonians of the system, respectively without and with the local perturbation. The system has n sites and at each site there are m orbitals. Therefore the summation in Eq. (9) is over the total of the nm orbitals in the system. Suppose the local perturbation affects only sites $l = 1,2,\ldots,k$; then we have $(EI-H_0)_i = (EI-H)_i$ for $i > km$, and Eq. (9) reduces to

$$\Delta N(E) = \sum_{i=1}^{km} \frac{\partial}{\partial E} \ln(\bar{G}^0_{i-1}/\bar{G}_{i-1}) \ . \tag{10}$$

Here we use the notation $\bar{G}^0_{i-1}$ and $\bar{G}_{i-1}$ to denote the (1,1) matrix elements of $[(EI-H_0)_i]^{-1}$ and $[(EI-H)_i]^{-1}$, respectively. The $\bar{G}^0_{i-1}$ and $\bar{G}_{i-1}$ are the Green's functions associated with the ith orbital in an unperturbed and perturbed system, respectively, with the first to $(i-1)$th orbitals missing. Equation (10) is greatly simplified when compared with Eq. (9) because we need only to evaluate km Green's functions instead of nm functions. The change of one-electron energies of the system under the local perturbation is

$$\Delta F = \int_{-\infty}^{E_F} (E-E_F)\Delta N(E) dE \ , \tag{11}$$

where $\int_{-\infty}^{E_F} dE$ represents the contour integral $(2\pi i)^{-1} \oint_c dE$ around a contour enclosing all the eigenvalues up to E_F.

Equation (11) has an especially simple form when we expand the $\bar{G}_i$ in terms of its zeros and poles in the following manner:

$$\bar{G}_i = \left[\prod_{l=1}^{L-1} (E-Z_{il})\right] \left[\prod_{l=1}^{L} (E-P_{il})^{-1}\right] \ , \tag{12}$$

where Z_{il} (P_{il}) are the zeros (poles) of $\bar{G}_i$. A similar expression holds for $\bar{G}^0_i$. We obtain

$$\frac{\partial}{\partial E} \ln \bar{G}_i = \sum_{l=1}^{L-1} (E-Z_{il})^{-1} - \sum_{l=1}^{L} (E-P_{il})^{-1} \ . \tag{13}$$

Equation (11) then has the following form:

$$\Delta F = -\sum_{i,l} Z_{il} + \sum_{i,l} P_{il} - (N_P - N_z)E_F + \sum_{i,l} Z^0_{il} - \sum_{i,l} P^0_{il} + (N^0_p - N^0_z)E_F \ . \quad (14)$$

Here N_p (N_z) and N_p^0 (N_z^0) are the total numbers of poles and zeros of $\sum_i \bar{G}_i$ and $\sum_i \bar{G}_i^0$, respectively, with energies below E_F. The sum over i in Eq. (14) is from 0 to $km-1$, and the sum over l is from 0 to L.

The numerical calculation of Eq. (14) can be performed by considering two fictitious densities of states $N^z(E)$ and $N^P(E)$ which contain all the correct poles and zeroes in Eq. (14), respectively. Thus the summations in Eq. (14) become the contour integrations $\int_{-\infty}^{E_F} EN^P(E)dE$ and $\int_{-\infty}^{E_F} EN^z(E)dE$ and can be evaluated via the recursion method.

The evaluation of Eq. (14) involves an integrated quantity and therefore requires a smaller value of the length L of the continued-fraction expansion than for the LDOS discussed above. For such integrated quantities it has been suggested that L should have a value related to the number of steps from the atom to the boundary.[17] We have performed an evaluation of the effect of L on the resulting change of energy of the system when one atom is removed from the system. When the central atom of a GaAs cluster (of size 512 atoms) is removed, the change of energy of the system, in addition to the energy of that atom at infinity, is shown in Fig. 3 as a function of the length L. The solid curve indicates the change when the central Ga atom is removed. The dashed curve is the change when a Ga atom occupying a site which is second-near neighbor to the central site is removed. For an infinitely large cluster these two curves should coincide. However, the two curves deviate from each other after $L > 10$ because the paths of the Hamiltonian interactions which reach the boundary from these two locations become different after $L > 10$. Both curves also become oscillating after $L > 10$. The curves shown in Fig. 3 are for $E_F = 0$. Because of the existence of a localized defect state in the gap for the Ga vacancy, the change of total electronic energy depends upon the position of E_F in the gap. In other words, it depends upon the doping and the filling of the defect states. From the above discussions for $E_F = 0$ we see that the boundary of the cluster introduces an uncertainty of energy ~ 0.02 eV in the results of the zeros-and-poles method when we use a 512-atom cluster and retain $L = 10$ coefficients. Therefore, meaningful results can be obtained only if the change of total energy due to local perturbation is greater than ~ 0.02 eV.

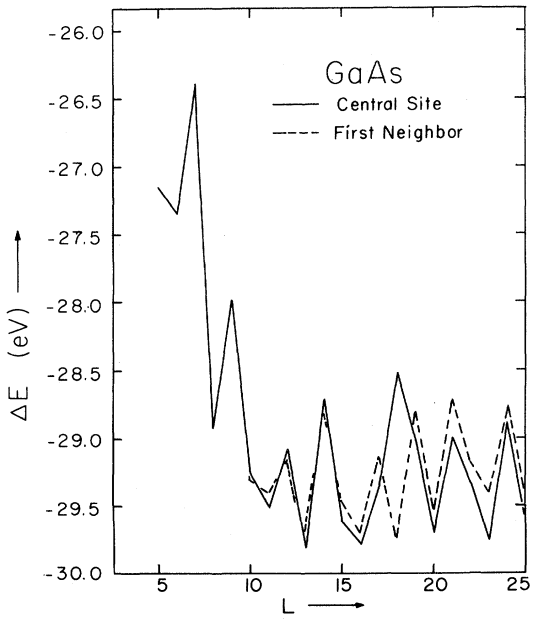

FIG. 3. Change of electronic energy vs the length of continued-fraction expansion when a Ga atom of a 512-atom cluster of GaAs is removed. Solid curve is for the Ga atom removed from the central site of the cluster. Dashed curve is for the Ga atom removed from second-neighbor to central site.

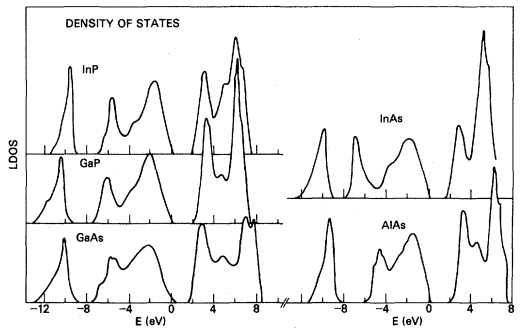

FIG. 4. DOS curves of pure GaAs, GaP, AlAs, InP, and InAs obtained by the present calculation.

III. RESULTS

A. Pure bulk crystals

Using the first- and second-nearest-neighbor Slater-Koster parameters of Osbourn and Smith[24] for GaAs and of Daw and Smith[25] for GaP, AlAs, InP, and InAs, we obtain the DOS curves shown in Fig. 4 for these systems. These results agree well with corresponding pseudopotential calculations.[22] The main difference between the two involves the sharpness of the Van Hove singularities. The finite-cluster calculations cannot reproduce this sharpness because the cancellation of the effects

TABLE I. Electron distributions at anion site A and cation site C in pure III-V semiconductors. $N_l^{(i)}$ denotes the number of electrons of l-type with energies lying in the ith valence band. N denotes the total number of electrons at a given site.

	GaAs	GaP	AlAs	InP	InAs
$N_s^{(1)}(A)$	1.43	1.47	1.53	1.58	1.49
$N_p^{(1)}(A)$	0.02	0.01	0.01	0.01	0.01
$N_s^{(1)}(C)$	0.29	0.24	0.24	0.13	0.13
$N_p^{(1)}(C)$	0.26	0.28	0.22	0.28	0.37
$N_s^{(2)}(A)$	2.87	3.07	2.90	3.12	3.03
$N_s^{(2)}(C)$	0.84	0.81	0.75	0.85	0.97
$N_p^{(2)}(C)$	2.15	1.98	2.16	1.93	1.87
$N(C)/N(A)$	0.80	0.71	0.75	0.67	0.73

from the cluster boundaries breaks down when the energy approaches Van Hove singularities. The present method also gives the LDOS for each orbital and hence gives the electron distribution for each band. In Table I, the results of the present calculations for the distributions of s and p electrons at anion and cation sites are given for the valence bands. As shown in Fig. 4, the valence bands of the III-V materials are separated into two parts by a heteropolar energy gap due to the potential difference between the two atoms in the unit cell. The lowest valence band for these materials is found to have s electrons concentrated more densely at the anion sites. This band is predominantly s-like about the anion atoms and s- and p-like about the cation atoms. For GaAs, the numbers of s and p electrons near the anion (cation) site are 1.43 and 0.02 (0.29 and 0.26), respectively. The second (upper) valence band is found to be much more covalent in character. The numbers of electrons on the anion and the cation sites are nearly equal for GaAs and are slightly different for GaP. This indicates that GaP is somewhat more ionic. The ionicity of these materials can be seen from the deviation of the last line in Table I from the value 0.6 for the perfectly ionic case. The corresponding values for pure AlAs, InP, and InAs are also listed in Table I for comparison.

The above results agree with the results of pseudopotential calculations[26] for the relative charge distribution near the anion and cation sites. In view of the above general agreement between the present results and the results of other calculations in the case of pure bulk crystals, we consider the sets of Slater-Koster parameters given in Refs. 24 and 25 as adequate to be used in the calculation of defect problems.

B. Ideal vacancies

Vacancies are expected to be common intrinsic defects in semiconductors. To date, there is little clear experimental evidence for the nature of the vacancy defects in III-V semiconductors. The type of vacancy defects (anion, cation, neutral, charged, monovacancy, or divacancy) depends on many conditions during the preparation and post-growth treatment of the crystal.

The ESR detected after 2-MeV electron irradia-

TABLE II. Energies of defect states introduced by cation vacancies V_c, anion vacancies V_a, anion antisite defects A_a, and cation antisite defects A_c in III-V semiconductors. Energies are in eV and are measured from the top of the valence bands. A_1 and T_2 denote the symmetries of the states. E_g is the energy gap in the pure materials.

		GaAs	GaP	AlAs	InP	InAs
E_g		1.52	2.35	2.11	1.41	0.37
	A_1	−9.03(−9.02)[a]	−9.42	−8.37	−8.92	−9.18
	A_1	−0.74(−0.60)[a]	−0.55	−0.60	−0.55	−0.54
V_c	T_2	0.44(0.63)[a]	0.44	0.81	0.44	0.27
	A_1	−9.99		−9.35		
	A_1	0.34		0.77		
V_a	T_2	1.21		1.58		
	A_1	−12.80	−13.10	−11.70	−11.10	−11.63
	A_1	−7.45	−7.77	−6.63	−8.11	−8.17
A_a	A_1	1.25	1.70	1.54	1.33	1.02
	A_1	−7.49		−5.79		
A_c	A_1	4.39		5.30		

[a]Numbers in parentheses are the energies when the atoms next to the vacancy are relaxed outward by 5%.

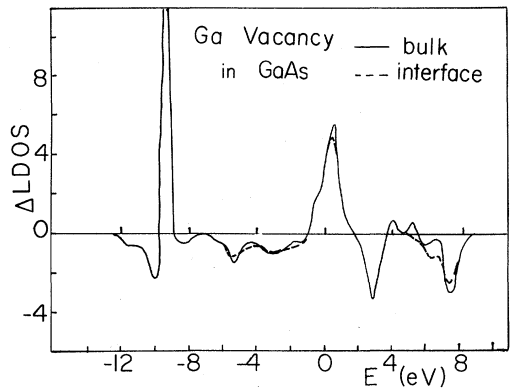

FIG. 5. Change of local density of states (ΔLDOS) evaluated at the anion site next to the cation vacancy in bulk GaAs (solid curve) and for a Ga vacancy next to GaAs-AlAs interface (dashed curve).

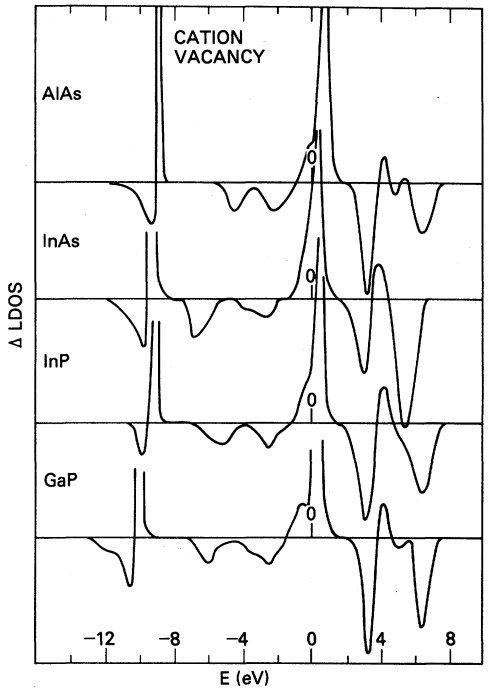

FIG. 6. ΔLDOS evaluated at the anion site next to the cation vacancy in AlAs, InAs, InP, and GaP.

tion of GaP was initially interpreted as due to the isolated Ga vacancy. Recently there have been questions about this identification because of disagreement with calculations.[11] It is therefore interesting to examine in detail vacancies in III-V materials. We have examined ideal cation vacancies in GaP, GaAs, InP, InAs, and AlAs and ideal anion vacancies in GaAs and AlAs. The positions and symmetries of major features of the electronic states of these defects are given in Table II and Figs. 5 and 6.

An ideal isolated cation vacancy (with no lattice relaxation) introduces bound states of symmetry T_2 in the lower parts of the energy gaps of these III-V semiconductors (except for InAs which has a small gap at 0.37 eV, and a T_2 state lying in midgap). The T_2 state is a dangling s-p hybrid which is predominantly p-like with a small s admixture at the first-nearest-neighbor anion sites. The percentage of p character of the T_2 state is 88.8% (83.7%) in GaP (GaAs). 76.1% (70.8%) of the electrons in this state in GaP (GaAs) are located at the first-near-neighbor sites indicating its highly localized character and justifying the use of the localized tight-binding approach in this calculation. The corresponding results for other III-V materials are listed in Table III. Three electrons occupy this level in the case of a neutral cation vacancy. When it is partially occupied, the T_2 state is subject to a symmetry-breaking Jahn-Teller-like distortion which will split the level and can change the charge state. We shall not consider this effect here.

Other major features of the ΔLDOS (the difference between the LDOS and that for the DOS in the bulk crystal) for ideal cation vacancies are a localized A_1 state near the top of the s-bonding band and an A_1 resonant state near the top of the valence

TABLE III. Percentage of p character of the T_2 states (n_p/n) and the percentage of electrons (n^{1st}/N) of the T_2 states located at first-neighbor sites of a cation vacancy or anion vacancy (subscript c or a) in III-V semiconductors.

	GaAs	GaP	AlAs	InP	InAs
$(n_p/n)_c$	0.84(0.873)[a]	0.89	0.89	0.89	0.89
$(n^{1st}/N)_c$	0.71(0.73)[a]	0.76	0.67		
$(n_p/n)_a$	0.65		0.70		
$(n^{1st}/N)_c$	0.58		0.71		

[a]Numbers in parentheses are the values when the atoms next to the vacancy are relaxed outward by 5%.

band. The former state is a purely s dangling-bond state localized primarily on the first-neighbor anion atom and extending slightly onto the neighbor; the latter is a resonant state mainly p-like about the first-near-neighbor anion (and second-near-neighbor cations).

We have also performed a calculation for a vacancy in GaAs with a 5% uniform outward dilation of the surrounding atoms. This relaxation results in a shift of the T_2 state to higher energy from 0.44 to 0.63 eV. This is equivalent to a change of $\Delta E(T_2)=1.56$ eV/Å for outward relaxation. The shift in energy of the gap state as a result of uniform dilation is relatively small and may be smaller than the splitting of the level due to the Jahn-Teller effect. The percentage of p character in the T_2 state increases to 87.31%, and 73.12% of the electrons in this state are located at the first-near-neighbor sites. This stronger p character and greater localization are a result of the lattice relaxation of the ligand site away from the center. The lower A_1 resonance state remains almost unchanged at -9 eV, but the higher A_1 resonance state moves to higher energy, $\Delta E(A_1)=1.7$ eV/Å. Thus the two A_1-symmetry states are pushed even farther apart while the T_2-A_1 splitting increases slightly from 1.18 to 1.23 eV. The positions of these levels are shown in Table II. These changes are similar to the changes calculated for the case of relaxed ligand atoms surrounding a Ga vacancy in GaP.[27] Also, the rate of change of the energy of A_1 and T_2 with dilation resembles the change of nitrogen-impurity levels in GaAs during dilation.[28] The ESR spectrum which has been interpreted as that of the cation vacancy in GaP has overall cubic symmetry.[1–4] It is a matter of current debate whether this ESR signal comes from the vacancy center or from a deep impurity center or if it results from rapid dynamical Jahn-Teller distortions associated with both T-symmetry phonons and E-symmetry phonons. (The former leads to a trigonal distortion and the latter to a tetragonal distortion.)

The states of the cation vacancies in the other III-V systems are similar to those in GaAs. Their features are given in Fig. 6 and Tables II and III.

We have also examined the arsenic vacancy in GaAs and AlAs. The positions and characters of the important structures in ΔLDOS for these cases are given in Tables II and III. The features of the ΔLDOS shown in Fig. 7 resemble those for the cation vacancy only in energy region near the gap. An ideal As vacancy introduces a T_2-symmetry state in the gap at an energy higher than that of the state in the gap for the cation vacancy. This gap state is formed by the s-p admixture of the dangling-bond states of the first-nearest-neighbor Ga atoms, and it is also highly localized at the first neighbors of the

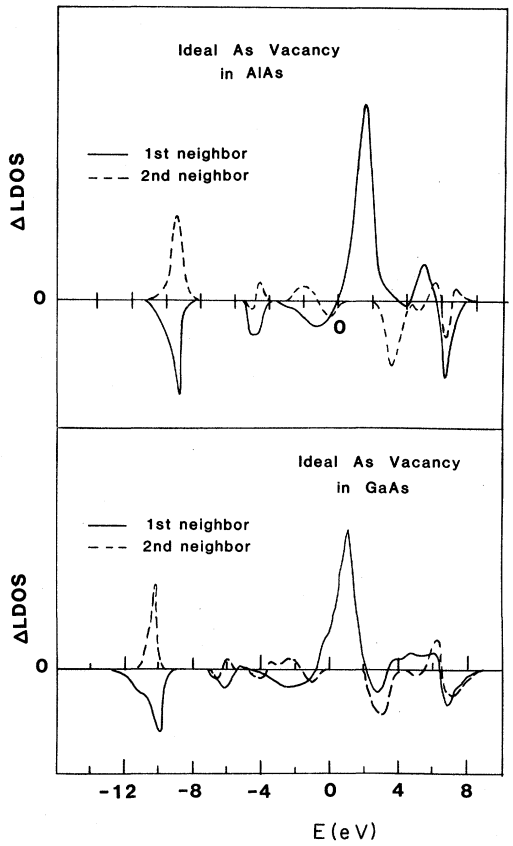

FIG. 7. ΔLDOS for anion vacancy in GaAs and AlAs. Solid curve evaluated at cation site next to the vacancy and dashed curve evaluated at the anion site which is the next near neighbor to the vacancy.

vacancy. However, unlike the T_2 state for the cation vacancy, the p-electron contribution to T_2 has decreased substantially (e.g., from 83.7% to 65.0% in GaAs). This is presumably due to the fact that the Ga (As) atom at the first-nearest-neighbor site has fewer (more) p electrons. For a neutral As vacancy, the T_2 level in the gap is occupied by one electron and, as with the case of the cation vacancy, it is unstable with respect to a Jahn-Teller distortion, which would lower its symmetry from that of the cubic case. To date, however, ESR corresponding to an anion vacancy has not been detected in the III-V semiconductors.

For these As vacancies a resonance state of A_1 symmetry is found to lie even closer to the valence-band edge than the corresponding resonance in the case of the cation vacancy. The lower A_1 resonant state near the top of the s-bonding band has quite different character from that in the cation vacancy. It is a resonant state for the second-nearest-neighbor orbitals and an antiresonant state for the first-nearest-neighbor orbitals because of the missing ar-

senic s-bonding electrons. This indicates that the s electrons redistribute and move from the first-near-neighbor sites to the second-neighbor sites to form bonding states instead of dangling-bond states at that energy.

Our results for the vacancy levels in general agree with calculations for GaP and GaAs by Scheffler *et al.*[11] and by Bernholc *et al.*,[27] except that the positions of our A_1 and T_2 states for the anion vacancy appear at lower energies. Our results for the A_1 and T_2 levels for cation vacancy appear at higher energies than their results. Our results, however, differ from those in several other calculations.[8,13,14] Srivastava finds an A_1 gap state for the anion vacancies in GaP and InP.[13] Madhukar and Das Sarma find both A_1 and T_2 gap states for cation vacancy in InAs.[14] Our results agree quantitatively with the calculations of Daw and Smith[25] who use the same set of tight-binding parameters. The results of our calculation for the ideal vacancies will not be compared with experiment here. The present calculations serve primarily to help to understand the properties of the antisite defects which are discussed in the next section.

C. *Antisite defects*

In studying the antisite defects we have examined several sets of interaction-matrix elements between the defect and its neighbors. For GaAs these include a set obtained from a fit to the band structure of bulk As and a set corresponding to these for bulk GaAs itself. The resulting LDOS has similar features for these choices. The relative positions of the localized states, however, differ somewhat. We believe that keeping the hopping-matrix elements for the antisite defect unaltered from the bulk is more reasonable than using matrix elements obtained from different tight-binding fits for different materials. The present calculations are done using the hopping-matrix elements of the pure crystal and varying only the site energies of the defect atom.

The results calculated here for ΔLDOS for anion antisite defects in the III-V semiconductors are given in Figs. 8 and 9. They exhibit three localized bound states, all of A_1 symmetry. There are A_1 states below and above the lower valence band and a state in the upper part of the gap (except for InAs). The physical origin of these states can be understood on the basis of a simple molecular model. In this model the defect anion is placed into an ideal cation vacancy, and the wave functions of the defect atom then hybridize with those of the ideal vacancy. The free-anion-atom s orbital hybridizes with the lowest A_1 resonance state of the cation vacancy and produces a bonding-antibonding pair of states below and above the s-bonding valence band. The upper A_1 resonant state of the vacancy is pushed up into the gap by interaction with the antisite s orbital and becomes a localized state in the upper part of the gap. For a neutral antisite defect, this A_1 gap state is occupied by two electrons. The T_2 gap state of the ideal vacancy interacts with the p orbital of the antisite defect state and forms two resonant states, one in the conduction band and one in the valence band.

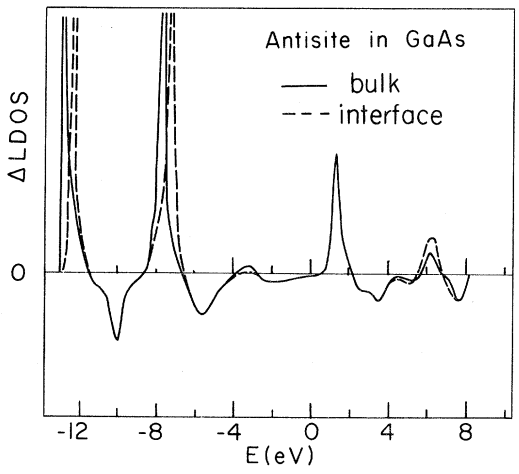

FIG. 8. ΔLDOS evaluated at the anion antisite in GaAs (solid curves) and at an anion antisite next to a GaAs-AlAs interface (dashed curve).

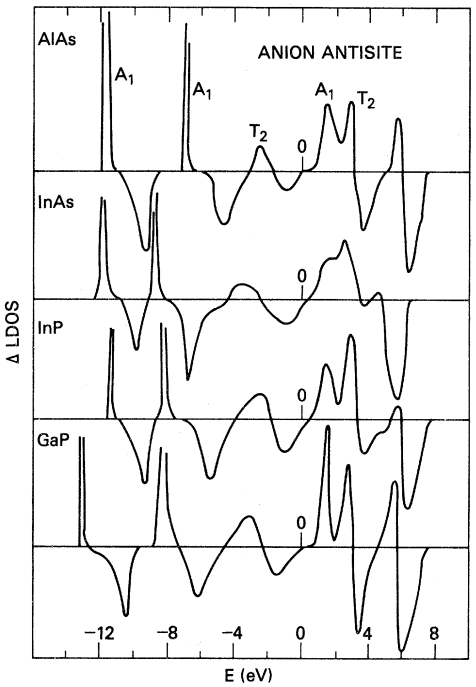

FIG. 9. ΔLDOS evaluated at the anion antisite in AlAs, InAs, InP, and GaP.

In the case of GaP the wave function of the A_1 gap state and the anion antisite contains 95.2% atomic s orbital. At the four ligand sites, the hybrid orbital, which is toward the central P site, has 80.9% p character. This value indicates that the bonding states have more p character than sp^3 even without relaxation of the ligands away from the central P site. Relaxation is usually caused by contributions from the antibonding character of the s orbital at the central site. Thus the outward relaxation which has been invoked to explain such hybridization observed in ESR measurements[1,4] is unnecessary. The p character of the localized gap state of the antisite is less than that of the ideal cation vacancy. We also find that 21.3% of the wave function of the A_1 gap state is at the central site, 58.8% is at the first-near-neighbor sites, and 18.9% is at the second-near-neighbor site. Therefore, most of the wave function is accounted for inside the second-near-neighbor shell, consistent with the fact that the A_1 state associated with the antisite is a well-localized state.

The antisite defect in GaAs has similar properties to that in GaP. There is an A_1 gap state at 1.25 eV above the valence-band edge. 14.9% of the wave function is at the central site, 44.8% is on the first-near-neighbor sites, and 39.8% is on second-near-neighbor sites, again indicating a highly localized state. At the central site the wave function has 87.0% atomic s character. At the ligand sites the wave function has 75.2% p character. For the case of GaAs, the p character has increased considerably compared with the case of GaP and approaches that of perfect sp^3 bonding. Because Ga has an atomic number closer to that of the As atom than that of the P, replacing the Ga atom by an As atom results in a smaller perturbation than replacing it by a P atom. Thus the antisite state is slightly more extended in GaAs than in GaP, and the distortion from sp^3 bonding is less pronounced for the antisite in GaAs than in GaP. Experiments are not yet accurate enough in the case of GaAs to determine whether there is any relaxation around the antisite defect. We have examined the effect of relaxations of the ligand atoms up to 8% of the lattice spacing for the antisite defect in GaAs. The resulting change of the defect gap state is only -0.10 eV. On the other hand, a decrease of the antisite self-energy by 0.68 eV changes the gap-state energy by -0.12 eV. From such studies we have found that the positions of gap states are relatively insensitive to the possible uncertainties in the site energies in the tight-binding Hamiltonians. Our present cation antisite defect level for GaP at 1.7 eV is closer to the levels determined by Jaros[12] and by Bernholz *et al.*[27] at 1.7–2.0 eV and 1.9 eV, respectively. Buisson *et al.*,[28] on the other hand, obtained 0.6 eV for GaP and 1.1 eV for GaAs. The latter values differ from our results because of the different tight-binding parameters being used. Buisson *et al.* considered only first-neighbor interactions but they included an excited s state as a basis state in their calculation.

TABLE IV. Electron distribution of A_1 gap state at anion antisite and its neighbors in III-V semiconductors. n_{si}, n_{pi}, n_{ti} denote the s, p, and total electron density at site i, respectively. $i = a,1,2$, for the anion site, first-neighbor site, and second-neighbor site.

	GaAs	GaP	AlAs	InP	InAs
(n_{sa}/n_{ta})	0.87	0.95	0.90	0.94	0.86
(n_{p1}/n_{t1})	0.75	0.81	0.84	0.82	0.86
$n_{ta}/2$	0.15	0.21	0.20	0.17	
$4n_{t1}/2$	0.45	0.59	0.65	0.48	
$12n_{t2}/2$	0.40	0.19			

Anion antisite defects in electron-irradiated, neutron-irradiated, or heavily-doped GaP and GaAs are now being detected experimentally by ESR.[1–7] These defects in other III-V semiconductors have not yet been observed, but they are expected to be present. Therefore, we also study these defects in AlAs, InP, and InAs. They exhibit features similar to those of anion antisite defects in GaP and GaAs. A summary of the positions of the defect levels is given in Table II and their electron distributions in Table IV. From Table II, we observe an interesting trend. The A_1 gap state of the anion antisite defect moves farther away from the valence-band edge as either the cation or the anion becomes lighter (that is, from InAs to GaAs,AlAs; from InP to GaP or from GaAs to GaP; from InAs to InP). This indicates that the s-like bonding state A_1 between the antisite defect and its neighbor deviates progressively from the p-like band state in the pure crystal when the cation or the anion becomes lighter. Presumably, this is caused by the progressive increase of s-electron contribution at the antisite to the A_1 level as shown in Table IV.

Recently Lagowski *et al.*[29] proposed that the EL2 level observed in deep-level transient spectroscopy (DLTS) in GaAs (0.82 eV below the conduction band in GaAs) could be associated with the anion antisite-defect level. From our results, the antisite-induced level in the gap is higher in energy than EL2. We shall consider an alternative possibility for EL2 in Sec. III D.

Cation antisite defects in GaP and GaAs so far have not been detected although they are believed to exist in GaSb (Ref. 8) and AlSb (Ref. 9). We have carried out calculations for cation antisite defects in AlAs and GaAs in order to investigate the possibili-

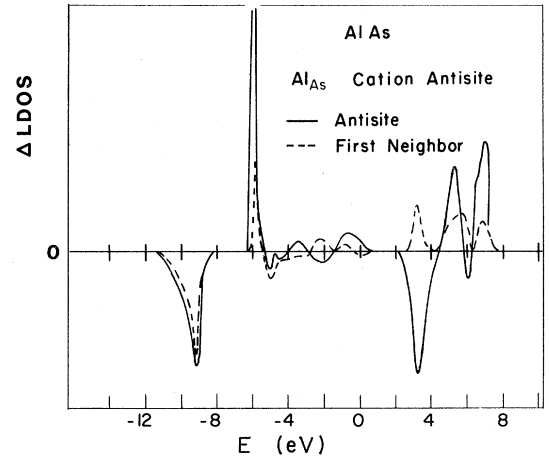

FIG. 10. ΔLDOS evaluated at the cation antisite (solid curve) and its near-neighbor site (dashed curve) in AlAs.

ty of a gap state in III-V semiconductors when the group-III element is lighter than the group-V element. The result is shown in Fig. 10 for AlAs. No gap state is found. A localized state of A_1 symmetry appears near the top of the s heteropolar gap. We interpret the cation antisite-induced states as coming from the interaction of As vacancy-induced states with the orbitals of the cation antisite. The cation atomic—s-oribital energy lies near the valence-band edge, and it interacts with the A_1 gap state of the anion vacancy. As a result, a localized "bonding" state at -5.79 eV is formed of A_1 symmetry just at the top of the heteropolar gap, and a resonant A_1 state appears in the conduction band at 5.30 eV. The Al p orbitals interact with the T_2 gap state of anion vacancy and create two resonant states, one in the valence band at -0.68 eV, the other in the conduction band at 7.18 eV. Several other resonant and antiresonant features also appear in the ΔLDOS of the antisite and the first-nearest-neighbor sites as shown in Fig. 10. Similar features are found for the cation antisite in GaAs.

The present results for the wave functions of the gap states for anion antisite defects in GaP and GaAs are consistent with recent ESR measurements as discussed in detail in Ref. 20(b). We note also that our results for the anion antisite defect in GaP are consistent with the calculations of Bernholc *et al.*[27] and of Jaros,[12] who used k-space Green's-function techniques with self-consistent and non-self-consistent pseudopotentials, respectively. We have considered here only the neutral defect. It is expected that, as in the case of the vacancy state in Si,[30] the positively charged state of the antisite defect lies below the neutral-defect state. More conclusive evidence concerning the charge state of the defect and the positions of the defect levels awaits further experimental work.

D. The ideal divacancy defect in GaAs

A divacancy defect in a III-V semiconductor is formed when a cation atom and one of its first-near-neighbor anion atoms are removed. In the case of Si, the divacancy defect has been found to be more stable than two single vacancies separated by one or more atoms.[31] It is suggested that this is true also in the case of GaAs. The divacancy defect in GaAs is particularly interesting because its properties are found to be consistent with the experimental results for EL2 level.[32] Although an alternative explanation for EL2 associated with the antisite defect was given by Lagowski *et al.*,[29] the gap-state energy level of the antisite defect obtained in the present calculation does not seem to be consistent with the observed position of EL2.

We have carried out a calculation for the deep levels of a divacancy defect in GaAs. Gap states are found at energies 0.13, 0.48, 0.82, and 1.17 eV above the valence-band edge. These states are related to the T_2 gap states for the single cation vacancy and the single anion vacancy. The 0.82-eV state corresponds better in energy to EL2 than does our result for the anion antisite. Sankey and Dow[28] have found a state at 0.9 eV for divacancy defect. An ideal divacancy defect lowers the symmetry of the crystal to trigonal symmetry, while an antisite defect does not alter the tetrahedral symmetry of the crystal. If this trap state can be detected by ESR, the symmetry analysis of the spectrum will determine whether EL2 is associated with a divacancy defect or an antisite defect. Unfortunately, experimental conditions for DLTS always require a highly conducting sample whereas ESR requires a highly insulating sample. Thus it is difficult to perform both experiments on the same sample. Our results with a gap state close to the energy of EL2 provide encouraging support for the suggestion that the divacancy defect may be associated with the EL2.

E. Defects near GaAs-AlAs interface

The GaAs-AlAs interface is technologically interesting and is a particularly attractive case for both experimental and theoretical investigation. It is known that GaAs-AlAs has perfect lattice matching. The valence-band discontinuity is also available experimentally. In the present calculations defects near an ideal (100) interface (IF) are considered, and the valence-band discontinuity is taken to be 0.035 eV, which has been used in previous theoretical in-

vestigations[33] and is similar to that observed experimentally on GaAs-$Al_xGa_{1-x}As$ heterostructures.[34]

In the present calculation, we choose a cluster of nearly cubic shape. The interface plane (IF plane) is a plane of As atoms with the Ga atoms of GaAs on one side and the Al atoms of AlAs on the other. There are alternatively eight and seven planes of atoms on each side of the IF plane. The site energies of the Al atoms have been decreased by 0.035 eV so as to produce the desired valence-band discontinuity. The site energies of the As atoms on the IF plane and the transfer-matrix elements between the As atoms along the IF plane are taken to be the average of these quantities in bulk GaAs and AlAs. The second-neighbor interaction-matrix elements between Al and Ga atoms across the IF are taken to be the average of Ga and Al in the respective bulks. We consider a defect in GaAs next to the IF plane. The defect-induced changes of the density of states ΔLDOS at the As site next to the Ga-vacancy defect is shown by the dashed curve in Fig. 5. The dashed curve in Fig. 8 is the result of ΔLDOS at an anion antisite next to the IF. It is seen that the IF causes only modest changes in the electronic states.

In order to investigate the interaction between defects and the interface, we use the zeros-and-poles method to calculate the changes in the total electronic energy of the As antisite and of the ideal vacancies as functions of position relative to the interace. The interaction energy of a defect with an interface arises from the sum of the energy changes from all parts of the LDOS of the system when the defect is placed near the interface. It involves both the localized states and extended states. Because of the complicated cancellations between the contributions of the various parts of the spectra, it is difficult to predict without calculations whether a given defect will be attracted to or repelled from the interface. The zeros-and-poles method allows the change of the integrals over the total density of states of the system to be carried out efficiently and accurately.

Our results show that the interaction energies of the defects with the IF are dependent on E_F, i.e., upon the filling of the gap states. For $E_F=0$, i.e., at the top of the valence band, the differences of the total electronic energies for defects on cation sites located in the plane adjacent to the IF less those three planes away from the IF are as follows: $\cong -0.06$ eV, for the cation vacancy in GaAs, and $\cong -0.10$ eV for the As antisite defect in GaAs. For $E_F=1.36$ eV, the gap states of the antisite defect and of the cation vacancy are filled. The corresponding changes of electronic energy at the above two positions are found to be larger: $\cong 1.1$ eV for the Ga vacancy, and $\simeq -0.15$ eV for the antisite defect. These results indicate that native defects may be attracted to or repelled from the interface during material formation or during processes involving defect motion, thus causing interface nonstoichiometry. The defect states may then pin Schottky barriers and affect other physical properties. We might note that nonstoichiometry at the IF of the GaAs-$Ga_xAl_{1-x}As$ heterostructures has been reported recently by Petroff *et al.*[35]

IV. SUMMARY

We have carried out the detailed theoretical investigation of native defects (vacancies and antisite defects) in the III-V semiconductors GaAs, GaP, InAs, AlAs, and InP, and near a model GaAs-AlAs interface using a large-cluster tight-binding recursion approach. The positions and symmetries of the defect-induced resonant states and localized states have been analyzed. It has been found that the character of the wave functions corresponding to the gap states in the forbidden gap are in agreement with the results of recent ESR experiments. A divacancy defect in GaAs has also been studied, and four gap states are found with one state at approximately the energy of EL2. The defect-interface interaction energies have been calculated by a generalized zeros-and-poles method. The results suggest that the defects may cause nonstoichiometry near the IF during formation because of the interaction.

ACKNOWLEDGMENTS

This work was supported in part by a U.S. Office of Naval Research contract. We would like to thank D. L. Smith and M. S. Daw for supplying us with their tight-binding Hamiltonians and for helpful comments concerning them.

[1]U. Kaufmann, J. Schneider, and A. Räuber, Appl. Phys. Lett. 29, 312 (1976).

[2]U. Kaufmann and T. A. Kennedy, J. Electron. Mater. 10, 347 (1981).

[3]U. Kaufmann, J. Schneider, R. Wörner, T. A. Kennedy, and N. D. Wilsey, J. Phys. C 14, L951 (1981).

[4]U. Kaufmann and J. Schneider, Festkörperprobleme 20, 87 (1980).

[5]T. A. Kennedy and N. D. Wilsey, in *International Conference on Radiation Effects in Semiconductors, Nice, 1978,* edited by J. H. Albany (IOP, London, 1979), p. 375.

[6]R. J. Wagner, J. J. Krebs, G. H. Stauss, and A. M. White, Solid State Commun. 36, 15 (1980); R. Wörner, U. Kaufmann, and J. Schneider, Appl. Phys. Lett. 40, 141 (1982).

[7]N. K. Goswami, R. C. Newman, and J. E. Whitehouse, Solid State Commun. 40, 473 (1981).

[8]Y. J. van der Meulen, J. Phys. Chem. Solids 28, 25 (1967); M. Jaros and S. Brand, Phys. Rev. B 14, 4494 (1976).

[9]R. Linnebach, K. W. Benz, and M. H. Pilkuhn, Verh. Dtsch. Phys. Ges. (VI) 15, 112 (1980).

[10]D. V. Lang, R. A. Logan, and L. C. Kimerling, Phys. Rev. B 15, 4874 (1977).

[11]M. Scheffler, S. T. Pantelides, N. O. Lipari, and J. Bernholc, Phys. Rev. Lett. 47, 413 (1981); J. Bernholc and S. T. Pantelides, Phys. Rev. B 18, 1780 (1978).

[12]M. Jaros, J. Phys. C 11, L213 (1978); M. Jaros and S. Brand, Phys. Rev. B 14, 4494 (1976).

[13]G. P. Srivastava, Phys. Status Solidi B 93, 761 (1979).

[14]A. Madhukar and S. Das Sarmas, J. Vac. Sci. Technol. 17, 1120 (1980).

[15]E. Kauffer, P. Pêcheur, and M. Gerl, J. Phys. C 9, 2319 (1976).

[16]T. A. Kennedy and N. D. Wilsey, Bull. Am. Phys. Soc. 27, 279 (1982).

[17]R. Haydock, V. Heine, and M. J. Kelley, J. Phys. C 8, 2845 (1975); in *Solid State Physics,* edited by H. Ehrenreich, F. Seitz, and D. Turnbull (Academic, New York, 1980), Vol. 35.

[18]N. P. Ilin and V. F. Masterov, Fiz. Tekh. Poluprovdn. 11, 1470 (1977) [Sov. Phys.—Semicond. 11, 864 (1978)]; V. F. Masterov and B. E. Samorukov, *ibid.* 12, 625 (1978) [*ibid.* 12, 363 (1978)].

[19]P. J. Lin-Chung and A. J. Holden, Phys. Rev. B 23, 3414 (1981).

[20](a) P. J. Lin-Chung and T. L. Reinecke, J. Vac. Sci. Technol. 19, 443 (1981); (b) T. L. Reinecke and P. J. Lin-Chung, Solid State Commun. 40, 285 (1981); (c) J. Luminescence 24/25, 355 (1981).

[21]L. A. Hemstreet, Phys. Rev. B 22, 4590 (1980); A. Fazzio and J. R. Leite, *ibid.* 21, 4710 (1980).

[22]G. A. Baraff and M. Schlüter, Phys. Rev. Lett. 41, 892 (1978).

[23]J. R. Chelikowsky and M. L. Cohen, Phys. Rev. B 14, 556 (1976).

[24]G. C. Osbourn and D. L. Smith, Phys. Rev. B 19, 2124 (1979).

[25]M. S. Daw and D. L. Smith, Phys. Rev. B 20, 5150 (1979) and private communication.

[26]J. P. Walter and M. L. Cohen, Phys. Rev. B 4, 1877 (1971).

[27]J. Bernholc, N. O. Lipari, S. T. Pantelides, and M. Scheffler, in *Proceedings of the 11th International Conference on Defects and Radiation Effects in Semiconductors, Oiso, 1980,* edited by B. R. Hasiguti (IOP, London, 1981), p. 1.

[28]C. A. Swarts, D. L. Miller, D. R. Franceschetti, H. P. Hjalmarson, P. Vogl, and J. D. Dow, Phys. Rev. B 21, 1708 (1980); H. P. Hjalmarson, P. Vogl, and D. J. Wolford, and J. D. Dow, Phys. Rev. Lett. 44, 810 (1980); J. P. Buisson, R. E. Allen, and J. D. Dow, J. Phys. (Paris) 43, 181 (1982); O. F. Sankey and J. D. Dow, Appl. Phys. Lett. 38, 685 (1981).

[29]J. Lagowski, H. C. Gatos, J. M. Parsey, K. Wada, M. Kaminska, and W. Walukiewicz, Appl. Phys. Lett. 40, 342 (1982).

[30]G. A. Baraff, E. O. Kane, and M. Schlüter, Phys. Rev. B 19, 4965 (1979).

[31]P. J. Lin-Chung and B. W. Henvis, Bull. Am. Phys. Soc. 27, 279 (1982).

[32]P. J. Lin-Chung in *Proceedings of the Materials Research Society Meeting, Boston, 1982* (in press).

[33]J. N. Schulman and T. C. McGill, Phys. Rev. B 19, 6341 (1979).

[34]R. Dingle, W. Wiegmann, and C. H. Henry, Phys. Rev. Lett. 33, 827 (1974).

[35]P. Petroff, C. Weisbuch, R. Dingle, A. C. Gossard, and W. Wiegmann, J. Vac. Sci. Technol 19, 571 (1981).